

Spin relaxation effects in the perpendicular magnetoresistance of magnetic multilayers

Albert Fert and Jean-Luc Duvail

Laboratoire de Physique des Solides, Université Paris-Sud, 91405 Orsay, France

Thierry Valet

Laboratoire Central de Recherches, Thomson-CSF, 91404 Orsay Cedex, France

(Received 30 January 1995)

The spin-diffusion length is the scaling length of the perpendicular giant magnetoresistance in magnetic multilayers and, according to recent experiments, the magnetoresistance ratio can be significantly reduced by enhancing the spin relaxation and thus shortening the spin-diffusion length. We present a theoretical picture of these spin-diffusion-length effects on the magnetoresistance. We also calculate the contribution from several mechanisms (spin-orbit scattering, exchange scattering by paramagnetic impurities, electron-magnon scattering) to the spin relaxation and spin-diffusion length.

I. INTRODUCTION

Since its discovery in 1988,^{1,2} the giant magnetoresistance (GMR) of the magnetic multilayers has generally been studied in the conventional CIP (current in the plane of the layers) geometry. Extension to the CPP (current perpendicular to the plane of the layers) geometry by Pratt and coworkers at Michigan State University dates from 1991.³⁻⁶ The first interest of the CPP geometry is that it leads to very high MR ratios, definitely higher than in the CIP geometry. This has been found in the Co/Cu and Co/Ag systems extensively investigated by Pratt *et al.*³⁻⁶ as well as in the Fe/Cr multilayers recently studied by Gijs, Lenczowski, and Giesbers,⁷ and this is probably very promising for applications. Also, on the fundamental side, the CPP-MR raises very interesting problems, as this has been recently discussed in several theoretical papers.⁸⁻¹³

An important point in most experimental results for Co/Cu and Co/Ag (Refs. 4-6) is the very simple variation of the magnetoresistance with the individual layer thicknesses. This variation has been accounted for by Lee and coworkers⁴⁻⁶ in a phenomenological picture of the CPP-MR. In a theory based on the Boltzmann equation, Valet and Fert¹³ have shown that this phenomenological picture can be justified rigorously when the spin-diffusion lengths ($l_{st}^{(N)}$ and $l_{st}^{(F)}$ in the normal and ferromagnetic layers, respectively) are much longer than the mean free paths and individual layer thicknesses (t_N and t_F). In the experimental conditions of Pratt *et al.*,³⁻⁶ i.e., for measurements in the helium temperature range, the spin-diffusion lengths are determined by the spin-orbit scattering and, in systems such as Co/Ag and Co/Cu, are expected to be relatively long, say above 1000 Å.¹³ Consequently, for most experiments of the Michigan State University group, the simple picture of the long spin-diffusion-length limit is certainly justified. However, other types of experiments have been recently performed; those of Gijs, Lenczowski, and Giesbers⁷ up to room temperature, and those of Yang *et al.*⁶ on Co/Ag and Co/Cu multilayers in which the Ag or Cu layers are doped with

magnetic impurities (Mn) or nonmagnetic impurities with strong spin-orbit interaction (Pt). These experiments raise problems related to the spin relaxation induced by magnons or impurities and to the behavior of the CPP-MR when such additional spin relaxation mechanisms make the spin-diffusion lengths shorter than the individual layer thicknesses. Our paper addresses these problems.

First, in Sec. II, we discuss the behavior of the CPP-MR out of the limit of very long spin-diffusion lengths. We show that, when the spin-diffusion lengths become shorter than the layer thicknesses, the CPP-MR is strongly reduced and no longer exhibits the simple variation with the layer thicknesses found for Co/Cu and Co/Ag.⁴⁻⁶ We have already discussed the influence of the spin-diffusion length in the nonmagnetic layer in two previous publications,¹² and our predictions have been compared with experimental results in Ref. 6. On the other hand, the results we present here on the influence of the spin-diffusion length in the magnetic layer have never been discussed.

In Secs. III and IV, we calculate the shortening of the spin-diffusion length expected from the addition of impurities with strong spin-orbit coupling (Sec. III) or paramagnetic impurities in the nonmagnetic layers (Sec. IV). The stronger effects (shortening of $l_{st}^{(N)}$ and reduction of the CPP-MR) are expected from paramagnetic impurities, in agreement with recent results of Yang *et al.*⁶

In Sec. V, we discuss the influence of temperature. First, in Sec. V A, we assume that, in spite of the additional spin relaxation arising from electron-magnon scattering, the spin-diffusion length is still much longer than the layer thickness. In these conditions, the CPP-MR is nevertheless reduced because the momentum transfer induced by spin-flip electron-magnon collisions (the so-called spin mixing mechanism) equalizes the spin-up and spin-down currents. We calculate this first contribution. Then, in Sec. V B, we estimate the second contribution arising from the shortening of the spin-diffusion length by electron-magnon scattering.

Finally we summarize our results data in Sec. VI.

II. CPP-MR OUT OF THE LIMIT OF VERY LONG SPIN-DIFFUSION LENGTHS

In a previous article,¹³ Valet and Fert (VF) concentrated on the behavior of the CPP-MR in the limit where the spin-diffusion lengths $l_{st}^{(N)}$ and $l_{st}^{(F)}$ are much longer than the layer thicknesses t_N and t_F . In this limit, the VF model leads to the simple expressions already used by Pratt *et al.*⁴⁻⁶ in a phenomenological analysis of their experimental data, that is to say

$$R^{(AP)} = M[\rho_F^* t_F + \rho_N^* t_N + 2r_b^*], \quad (1)$$

$$R^{(P)} = R^{(AP)} - \frac{\left[\beta \rho_F^* \frac{t_F}{t_F + t_N} L + 2\gamma r_b^* M \right]^2}{R^{(AP)}}, \quad (2)$$

$$\sqrt{(R^{(AP)} - R^{(P)})R^{(AP)}} = \beta \frac{t_F}{t_F + t_N} \rho_F^* L + 2\gamma r_b^* M, \quad (3)$$

where $R^{(AP)}$ and $R^{(P)}$ are the resistances of a unit area of the multilayer for the antiparallel (or random) and parallel arrangements, respectively, ρ_N^* is the resistivity of the normal layers, $\rho_{\uparrow(\downarrow)} = 2\rho_F^*[1 - (+)\beta]$ are the resistivities of the spin \uparrow and spin \downarrow channels in the ferromagnetic layers, $r_{\uparrow(\downarrow)} = 2r_b^*[1 - (+)\gamma]$ are the resistances of the F/N interfaces for the spin \uparrow and spin \downarrow channels, t_F and t_N are the thicknesses of the F and N layers, respectively, M is the number of bilayers, and $L = M(t_F + t_N)$ is the total thickness of the structure. The right-hand side of Eq. (3) includes two contributions respectively due to bulk and interface spin dependent scattering: the first one is the product of the total resistance of the magnetic layers ($\rho_F^* L t_F / [t_F + t_N]$) or, as written by Pratt *et al.*^{5,6} $M t_F \rho_F^*$ by their asymmetry coefficient β ; the second one is the product of the resistance of the interfaces ($2M r_b^*$) by their asymmetry coefficient γ .

In the usual conditions of Pratt *et al.*,⁴⁻⁶ L is constant and Eq. (3) leads to a linear variation as a function of the number of bilayers M . In the case of structures with equal thicknesses for the magnetic and normal layers, i.e., $t_F = t_N = L/2M$, Eq. (3) becomes

$$\sqrt{(R^{(AP)} - R^{(P)})R^{(AP)}} = \beta \rho_F^* \frac{L}{2} + 2\gamma r_b^* M. \quad (4)$$

In the case where L and t_F are constant and $t_N = (L - M t_F)/M$, Eq. (3) becomes

$$\sqrt{(R^{(AP)} - R^{(P)})R^{(AP)}} = [\beta t_F \rho_F^* + 2\gamma r_b^*] M. \quad (5)$$

These two types of linear variations with M , calculated with values of $\beta, \gamma, \rho_F^*, r_b^*, L, t_F$ used in the fits of experimental results on Co/Ag multilayers by Pratt and co-workers,^{5,6} are the straight lines in Figs. 1(a) and 1(b). We recall that Eqs. (1)–(5) hold only for $l_{st}^{(F)} \gg t_{N(F)}$, so that the linear variations continuing down to $M = 1$ in Fig. 1 are expected only for $M \gg L/l_{st}^{(F)}$.

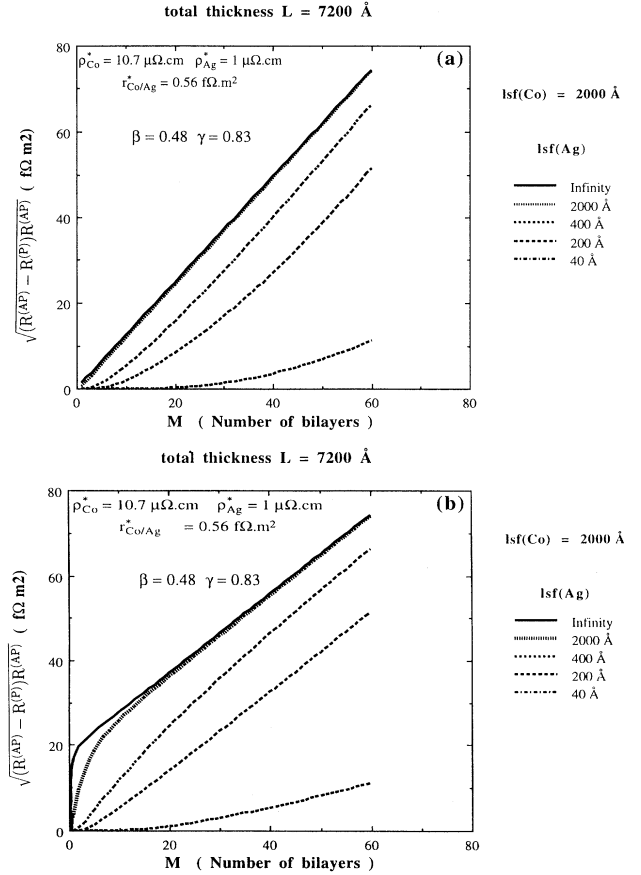


FIG. 1. Influence of a reduction of the spin-diffusion length in the nonmagnetic layers on the square root plots: for a Co/Ag multilayer with a fixed total thickness, $L = 7200 \text{ \AA}$, $\sqrt{[R^{(AP)} - R^{(P)}]R^{(AP)}}$ is plotted as a function of the number of bilayers M for several values of $l_{sf}^{(Ag)}$, indicated on the figure. The parameters of the calculation from Eqs. (6)–(8) are those derived from measurements on Co/Ag,^{5,6} i.e., $\rho_{Ag}^* = 1 \mu\Omega \text{ cm}$, $\rho_{Co}^* = 10.7 \mu\Omega \text{ cm}$, $r_b^* = 0.56 \text{ f}\Omega \text{ cm}^2$, $\beta = 0.48$, $\gamma = 0.83$, with also $l_{sf}^{(Co)} = 2000 \text{ \AA}$ for the spin diffusion length in the magnetic layers. (a) is for $t_{Co} = 60 \text{ \AA}$, $t_{Ag} = L/M - t_{Co}$ [as in Figs. 1 and 3 from Yang *et al.* (Ref. 6)]; (b) is for $t_{Co} = t_{Ag} = L/(2M)$ [conditions chosen in the upper Fig. 3 of Pratt *et al.*, Ref. 5]. The linear variations shown for infinite $l_{sf}^{(Ag)}$ are those predicted by Eq. (5). The curves for finite $l_{sf}^{(Ag)}$ are somewhat different from those published by Fert *et al.* (Fig. 1 in Ref. 12) or Yang *et al.* (Figs. 1 and 3 in Ref. 6) because we have kept the resistivity of pure Ag layers. In contrast, the curves of Refs. 12 and 6 were calculated to account for experimental results on Co/AgPt multilayers and used the resistivity of AgPt alloys. This does not change significantly the results.

Now, suppose that additional spin relaxation mechanisms (impurities, magnons) shorten the spin-diffusion lengths to values of the order of magnitude of the layer thicknesses. Then Eqs. (1)–(5) are no longer valid and have to be replaced by the general expressions of $R^{(AP)}$ and $R^{(P)}$, Eqs. (40)–(43) in Ref. 13, i.e.,

$$R^{(P,AP)} = M[r_0 + 2r_{\text{SI}}^{(P,AP)}] \text{ with } r_0 = (1 - \beta^2)\rho_F^* t_F + \rho_N^* t_N + 2(1 - \gamma^2)r_b^*, \quad (6)$$

$$r_{\text{SI}}^{(P)} = \frac{\frac{(\beta - \gamma)^2}{\rho_N^* l_{\text{sf}}^{(N)}} \text{Coth} \left[\frac{t_N}{2l_{\text{sf}}^{(N)}} \right] + \frac{\gamma^2}{\rho_F^* l_{\text{sf}}^{(F)}} \text{Coth} \left[\frac{t_F}{2l_{\text{sf}}^{(F)}} \right] + \frac{\beta^2}{r_b^*}}{\frac{1}{\rho_N^* l_{\text{sf}}^{(N)}} \text{Coth} \left[\frac{t_N}{2l_{\text{sf}}^{(N)}} \right] + \frac{1}{\rho_F^* l_{\text{sf}}^{(F)}} \text{Coth} \left[\frac{t_F}{2l_{\text{sf}}^{(F)}} \right] + \frac{1}{r_b^*} \left\{ \frac{1}{\rho_N^* l_{\text{sf}}^{(N)}} \text{Coth} \left[\frac{t_N}{2l_{\text{sf}}^{(N)}} \right] + \frac{1}{\rho_F^* l_{\text{sf}}^{(F)}} \text{Coth} \left[\frac{t_F}{2l_{\text{sf}}^{(F)}} \right] \right\}}, \quad (7)$$

$$r_{\text{SI}}^{(AP)} = \frac{\frac{(\beta - \gamma)^2}{\rho_N^* l_{\text{sf}}^{(N)}} \text{Tanh} \left[\frac{t_N}{2l_{\text{sf}}^{(N)}} \right] + \frac{\gamma^2}{\rho_F^* l_{\text{sf}}^{(F)}} \text{Coth} \left[\frac{t_F}{2l_{\text{sf}}^{(F)}} \right] + \frac{\beta^2}{r_b^*}}{\frac{1}{\rho_N^* l_{\text{sf}}^{(N)}} \text{Tanh} \left[\frac{t_N}{2l_{\text{sf}}^{(N)}} \right] + \frac{1}{\rho_F^* l_{\text{sf}}^{(F)}} \text{Coth} \left[\frac{t_F}{2l_{\text{sf}}^{(F)}} \right] + \frac{1}{r_b^*} \left\{ \frac{1}{\rho_N^* l_{\text{sf}}^{(N)}} \text{Tanh} \left[\frac{t_N}{2l_{\text{sf}}^{(N)}} \right] + \frac{1}{\rho_F^* l_{\text{sf}}^{(F)}} \text{Coth} \left[\frac{t_F}{2l_{\text{sf}}^{(F)}} \right] \right\}}. \quad (8)$$

The spin-diffusion length in the nonmagnetic layers, $l_{\text{sf}}^{(N)}$, is related to the spin mean free path $\lambda_{\text{sf}}^{(N)}$ and momentum mean free path $\lambda^{(N)}$ by¹³

$$l_{\text{sf}}^{(N)} = \left[\frac{\lambda^{(N)} \lambda_{\text{sf}}^{(N)}}{6} \right]^{1/2}. \quad (9)$$

The spin-diffusion length of the magnetic layers, $l_{\text{sf}}^{(F)}$, is related to the momentum mean free paths λ_{\uparrow} and λ_{\downarrow} , and the spin mean free path $\lambda_{\text{sf}}^{(F)}$ by

$$l_{\text{sf}}^{(F)} = \left[\frac{\lambda_{\uparrow} \lambda_{\downarrow} \lambda_{\text{sf}}^{(F)}}{3(\lambda_{\uparrow} + \lambda_{\downarrow})} \right]^{1/2}. \quad (10)$$

We will first consider how shortening $l_{\text{sf}}^{(N)}$ reduces the MR and distorts the linear variation of $\sqrt{(R^{(AP)} - R^{(P)})R^{(AP)}}$ with M found in the limit of very long spin-diffusion lengths.

We have calculated $\sqrt{(R^{(AP)} - R^{(P)})R^{(AP)}}$ from Eqs. (6)–(8) with the parameters of the fit by Pratt and co-workers for Co/Ag,⁵ with a very long $l_{\text{sf}}^{(F)}$ (2000 Å) and with different values of $l_{\text{sf}}^{(N)}$ between infinity and 20 Å. As shown in Fig. 1, the MR is rapidly reduced as $l_{\text{sf}}^{(N)}$ is shortened. For a given value of $l_{\text{sf}}^{(N)}$, the variation of $\sqrt{(R^{(AP)} - R^{(P)})R^{(AP)}}$ with M is no longer linear: it starts with a positive curvature (in fact exponentially, as $\exp[-L/(4Ml_{\text{sf}}^{(N)})]$) at small values of M in Fig. 1 and catches up with the linear variation of the long spin-diffusion-length limit for $M \gg L/l_{\text{sf}}^{(N)}$. Such a behavior has been recently observed by Yang *et al.*⁶ in Co/Ag and Co/Cu multilayers in which Mn or Pt impurities have been introduced in the silver layers to shorten their spin-diffusion length. By fitting Eqs. (6)–(8) with their experimental results, they have determined the spin diffusion length $l_{\text{sf}}^{(N)}$ for each concentration of Mn or Pt. For example, $l_{\text{sf}}^{(N)}$ is reduced to 2.8 nm by the addition of 7% of Mn in Cu.⁶

Equations (6)–(8) can also be used to predict how the CPP-MR is reduced by shortening the spin-diffusion length in the ferromagnetic layers, $l_{\text{sf}}^{(F)}$. In Fig. 2 we show plots of $\sqrt{(R^{(AP)} - R^{(P)})R^{(AP)}}$ versus M calculated again with the parameters of the fit by Pratt and co-workers for Co/Ag, with now $l_{\text{sf}}^{(N)} = 5000$ Å and several “short” values of $l_{\text{sf}}^{(F)}$. We see that shortening $l_{\text{sf}}^{(F)}$ also reduces the MR and distorts the linear variation of the

long spin-diffusion-length limit. The curves start from zero with a negative curvature and catch up with the linear variation for $M \gg L/l_{\text{sf}}^{(F)}$. In contrast with the exponential variation at small M , when $l_{\text{sf}}^{(F)}$ is shortened, the variation at small values of M is linear in M .

III. INFLUENCE OF SPIN-ORBIT SCATTERING BY IMPURITIES

The case of spin flip scattering by impurities I with strong spin-orbit interaction ($I = \text{Au, Pt, or other } 5d \text{ elements, also Pb or Bi}$) is relatively simple. Spin-orbit scattering by such impurities brings an additional and temperature independent contribution to the spin relaxation.¹⁴ The total spin relaxation rate will be written as

$$\frac{1}{\tau_{\text{sf}}} = \frac{1}{\tau_{\text{sf}}^{(0)}} + \frac{1}{\tau_{\text{sf}}^{(I)}}, \quad (11)$$

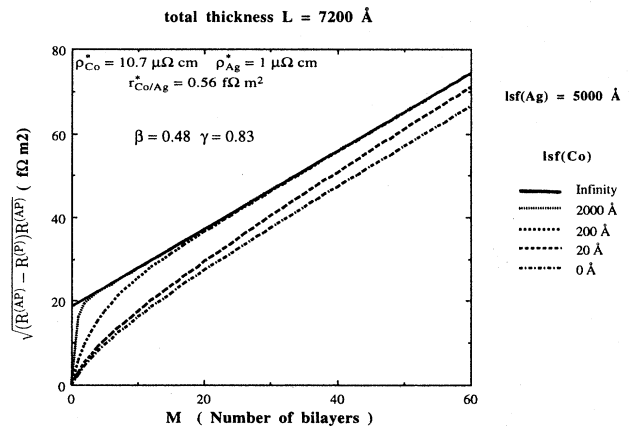


FIG. 2. Same caption as for Fig. 1(b) but now for a fixed value $l_{\text{sf}}^{(\text{Ag})} = 5000$ Å and several values of $l_{\text{sf}}^{(\text{Co})}$ indicated on the figure. According to the experimental square root plots of Pratt *et al.* (Ref. 5), a linear variation is observed down to $M = 10$ (thickest Ag layers in the samples of Ref. 5). Only our curves for $l_{\text{sf}}^{(\text{Co})} > 200$ Å keep a linear variation down to $M = 10$, and thus we can conclude that the actual spin-diffusion length in the Co layers is longer than 200 Å.

where $1/\tau_{sf}^{(0)}$ is due to spin-orbit scattering by defects and residual impurities, while $1/\tau_{sf}^{(I)}$ is due to spin-orbit scattering by the impurities I and proportional to their concentration N_I per unit volume (we consider the low temperature limit and will treat the additional contribution from electron-magnon scattering only in Sec. VB). For transition metal impurities, the spin-orbit scattering is due mainly to the hybridization between the conduction band states and the d states of the impurity, in other words to the formation of a virtual bound state.^{14,15} This leads to simple expressions of the spin flip cross section $\sigma_{sf}^{(I)}$ and relaxation time¹⁵:

$$\sigma_{sf}^{(I)} = \frac{40\pi}{k_F^2} \left[\frac{\lambda_d}{\Delta} \right]^2 \sin^2 \left[\pi \frac{Z_d}{10} \right], \quad (12)$$

$$\frac{1}{\tau_{sf}^{(I)}} = N_I v_F \sigma_{sf}^{(I)}, \quad (13)$$

where λ_d is the spin orbit constant of the d states, Δ is the width of the virtual bound state (≈ 1 eV), Z_d is the number of d electrons, and k_F and v_F are the Fermi wave vector and velocity, respectively. Note that Eq. (12) is for nonmagnetic transition metal impurities.

Large spin-flip cross sections are expected for transition metal impurities at the end of the $5d$ series for which λ_d is much stronger than for $3d$ or $4d$ elements [for example, $\lambda_d \approx 0.51$ eV for Pt against $\lambda_d \approx 0.076$ eV for Ni (Ref. 16)]. For Pt in Cu the spin flip cross section is known from electron spin resonance (ESR) experiments, $\sigma_{sf} \approx 4.0 \times 10^{-17}$ cm² (Refs. 14 and 17) and, for a given concentration of Pt, this cross section can be converted into spin mean free path from Eq. (13). Suppose, for example, Cu layers containing 6 at. % of Pt impurities: starting from the above value of σ_{sf} and neglecting $1/\tau_{sf}^{(0)}$ [that is assuming $\lambda_{sf} = \tau_{sf}^{(I)} v_F = [N_I \sigma_{sf}^{(I)}]^{-1}$ from Eq. (13)], a straightforward calculation leads to $\lambda_{sf} \approx 500$ Å. Assuming a resistivity of 13 $\mu\Omega$ cm for Cu + 6 at. % Pt,^{6,18} we also obtain $\lambda = 55$ Å and, from Eq. (9):

$$I_{sf}^{(N)} = 68 \text{ Å}. \quad (14)$$

This is the value also derived by Yang *et al.*⁶ By fitting their experimental data with the VF theory (see Fig. 4 in Ref. 6), they have found a good fit for $I_{sf}^{(N)} = 80$ Å, which is in good agreement with the above 68 Å. Larger spin flip cross section and shorter $1_{sf}^{(N)}$ can be expected with Os or Ir impurities [larger value of $\sin(\pi Z_d/10)$].

We finally point out that Eq. (12) holds only for transition metal impurities. The calculation of σ_{sf} is more complex for sp elements.¹⁴ However, there are ESR experimental data for some impurities, for example, $\sigma_{sf} = 2.0 \times 10^{-17}$ cm² and $\sigma_{sf} = 2.5 \times 10^{-17}$ cm² for Au impurities in Cu and Ag, respectively, which is definitely smaller than for Pt impurities, 4.0×10^{-17} cm² in Cu and 9.3×10^{-17} cm² in Ag, respectively.^{17,19}

Equation (12) can also be used to estimate the spin relaxation rate in "nondoped" multilayers such as Co/Cu or Co/Ag. The spin flip scattering is then by the spin orbit part of the scattering potential of defects or interdiffused atoms. Therefore the involved spin orbit in-

teraction is that of Co, Cu, or Ag, which leads to a ratio larger than 10^2 between the non-spin-flip or spin-flip cross sections. For mean free path longer than 10^2 Å, this also leads to spin-diffusion length longer than 10^3 and therefore justifies the simple expressions used by Pratt *et al.*^{5,6} to interpret experimental results on Co/Ag and Co/Cu. Similar estimates by Yang *et al.*⁶ lead to 5000 and 4500 Å for the spin-diffusion lengths of Ag and Cu layers, respectively.

IV. INFLUENCE OF SPIN FLIP SCATTERING BY EXCHANGE INTERACTIONS WITH PARAMAGNETIC IMPURITIES

Recent experiments on Cu/Ag and Co/Cu multilayers with Mn impurities in the nonmagnetic layers have shown that the CPP-MR is strongly reduced by Mn impurities.⁶ In this section, we calculate the influence of exchange spin-flip scattering by such paramagnetic impurities on the spin-diffusion length.

Compared to the case of spin-orbit scattering (Sec. III), the problem of the spin-flip scattering by exchange interaction with paramagnetic impurities is a little more complex because exchange scattering does not relax the spin accumulation directly to the lattice but transfers it to the paramagnetic impurity system. This problem of relaxation via paramagnetic impurities is similar to that of electron spin resonance in dilute magnetic alloys and we adopt the conventional notation of ESR: $1/\tau_{sd}$ is the spin relaxation rate of the conduction electrons towards the paramagnetic impurities, $1/\tau_{ds}$ is the spin relaxation rate of the paramagnetic impurities towards the conduction electrons (the so-called Korringa rate), $1/\tau_{sl}$ and $1/\tau_{dl}$ are the respective spin relaxation rate of the conduction electrons and paramagnetic impurities to the lattice (the relaxation rate $1/\tau_{sl}$ of the ESR is twice the spin flip rate $1/\tau_{sf}$ of the preceding section²⁰). When the exchange interaction between the spin s of a conduction electron and the spin S of a paramagnetic impurity is written as

$$H_{\text{exch}} = -2Js \cdot S \delta(r), \quad (15)$$

the classical expression for $1/\tau_{sd}$ and $1/\tau_{ds}$ are^{21,22}

$$\frac{1}{\tau_{sd}} = \frac{8}{3} \frac{\pi}{\hbar} N_I S(S+1) J^2 n(E_F), \quad (16)$$

$$\frac{1}{\tau_{ds}} = 4\pi [Jn(E_F)]^2 k_B T, \quad (17)$$

where N_I is the number of magnetic impurities per unit volume, S is the spin of the paramagnetic impurities, and $n(E_F)$ is the density of states at the Fermi level per unit volume and per spin direction.

In the presence of both spin-lattice and s - d relaxations for the conduction electrons, the balance between the spin accumulation related to current gradients and the spin relaxation is written

$$\frac{\mu_B}{e} \left[\frac{dJ_+}{dz} - \frac{dJ_-}{dz} \right] = \left[\frac{1}{\tau_{sl}} + \frac{1}{\tau_{sd}} \right] \Delta M_s - \frac{\Delta M_d}{\tau_{ds}}. \quad (18)$$

J_+ and J_- are the current densities for the two spin directions, z is the axis perpendicular to the layers, and ΔM_s and ΔM_d are the out of equilibrium magnetizations for the conduction electrons and magnetic impurities. Equation (18) is similar to the first of Eqs. (13) in Ref. 13; in fact, with $1/\tau_{sd}=1/\tau_{ds}=0$, Eq. (18) would be reduced to the corresponding equation of Ref. 13.

For the impurity spins, there is no spin accumulation term related to current gradients and there is only balance between sd , ds , and dl relaxation terms:

$$0 = \left[\frac{1}{\tau_{dl}} + \frac{1}{\tau_{ds}} \right] \Delta M_d - \frac{\Delta M_s}{\tau_{sd}}. \quad (19)$$

Combining Eqs. (18) and (19) leads to

$$\frac{\mu_B}{e} \left[\frac{dJ_+}{dz} - \frac{dJ_-}{dz} \right] = \left[\frac{1}{\tau_{sl}} + \frac{1}{\tau_{sd}} \left(\frac{\tau_{ds}}{\tau_{ds} + \tau_{dl}} \right) \right] \Delta M_s. \quad (20)$$

We thus find that, in addition to the spin-orbit term of direct relaxation to the lattice, i.e., $1/\tau_{sl}$, there is an additional contribution to the spin relaxation provided by the exchange scattering. When we use Eq. (16) to express $1/\tau_{sd}$, this exchange contribution to $1/\tau_{sf}$ is written as²⁰

$$\left[\frac{1}{\tau_{sf}} \right]^{\text{exch}} = \frac{4\pi N_I S(S+1) J^2 n(E_F)}{3\hbar} \frac{\tau_{ds}}{\tau_{ds} + \tau_{dl}}. \quad (21)$$

In the low temperature limit, according to Eq. (17) for the Korringa rate, $1/\tau_{ds}$ tends to zero, so that

$$\left[\frac{1}{\tau_{sf}} \right]^{\text{exch}}_{\text{low } T} = \left[\frac{1}{\tau_{sf}} \right]^{\text{exch}}_{\text{max}} = \frac{4\pi N_I S(S+1) J^2 n(E_F)}{3\hbar}. \quad (22)$$

As temperature increases, the Korringa rate increases so that $(1/\tau_{sf})^{\text{exch}}$ decreases below its low temperature value given by Eq. (22). This shows that the efficiency of paramagnetic impurities for shortening the spin-diffusion length and for reducing the CPP-MR is expected to decrease with temperature.

For a numerical illustration, we choose the example of Cu layers doped with Mn impurities. We can derive the spin-flip rate from magnetotransport data. We assume an impurity scattering potential of the form

$$H_{\text{scat}} = (V - 2\mathbf{J}\mathbf{s}\cdot\mathbf{S})\delta(\mathbf{r}) \quad (23)$$

so that the resistivity relaxation rate is written as

$$\left[\frac{1}{\tau} \right]^{\text{res}} = \frac{2\pi N_I}{\hbar} [V^2 + S(S+1)J^2] n(E_F) \quad (24a)$$

and is related to the low temperature spin relaxation rate, Eq. (22), by

$$\left[\frac{1}{\tau_{sf}} \right]^{\text{exch}}_{\text{low } T} / \left[\frac{1}{\tau} \right]^{\text{res}} = \frac{2}{3} \frac{S(S+1) \left(\frac{J}{V} \right)^2}{1 + S(S+1) \left(\frac{J}{V} \right)^2}. \quad (24b)$$

Taking the value $J/V=0.133$ derived from magne-

toresistance measurements on CuMn alloys²³ and $S=5/2$, we obtain

$$\left[\frac{1}{\tau_{sf}} \right]^{\text{exch}}_{\text{low } T} / \left[\frac{1}{\tau} \right]^{\text{res}} = 0.089. \quad (25)$$

According to ESR data for CuMn, the additional spin-flip scattering rate by the spin orbit of Mn is much smaller¹⁴ and will be neglected here, i.e., we take

$$\left[\frac{1}{\tau_{sf}} \right]^{\text{exch}}_{\text{low } T} = \left[\frac{1}{\tau_{sf}} \right]^{\text{exch}}_{\text{low } T} = 0.089 \left[\frac{1}{\tau} \right]^{\text{res}}. \quad (26)$$

Supposing 7 at. % of Mn impurities in Cu, taking ρ (7% Mn) = $31 \mu\Omega \text{ cm}$ (Ref. 18) and 1 free electron per atom in the conduction band of Cu, we obtain that the corresponding mean free path is

$$\lambda^{(N)} = 21 \text{ \AA}. \quad (27)$$

Then, from Eq. (26):

$$\lambda_{\text{sf}}^{(N)} = \lambda^{(N)} / 0.089 = 236 \text{ \AA}. \quad (28)$$

The spin-diffusion length is then derived from Eq. (9),

$$l_{\text{sf}}^{(N)} = \frac{\sqrt{\lambda_{\text{sf}}^{(N)} \lambda^{(N)}}}{6} = 29 \text{ \AA}. \quad (29)$$

Out of the low temperature limit, the Mn impurities are expected to be less efficient as Eq. (22) has to be replaced by Eq. (21), which includes the reduction factor $\tau_{ds}/(\tau_{ds} + \tau_{dl})$. We can rapidly check that 4.2 K is not strictly in the low temperature limit. According to ESR data, $\gamma(1/\tau_{dl})$ (with $\gamma=2\mu_B/h$) is around 200 G in implanted CuMn alloys, while $\gamma(1/\tau_{ds})/T=45 \text{ G K}^{-1}$.²⁴ This leads to a reduction factor of 0.51 for $(1/\tau_{sf})^{\text{exch}}$ at 4.2 K and to a value around 40 \AA for $l_{\text{sf}}^{(N)}$. Spin glass freezing could also freeze out a part of the spin flip and increase $l_{\text{sf}}^{(N)}$ a little more.

In the CPP experiments on CuMn(7%)/Co, a good fit with the VF model has been obtained by Yang *et al.*⁶ with $l_{\text{sf}}^{(N)}=28 \text{ \AA}$. This is in better agreement with the nonreduced value of 29 \AA, Eq. (29), and suggests that, at 4.2 K, the reduction factor is less important than we have estimated. However, the reduction must become really effective at higher temperature.

V. INFLUENCE OF TEMPERATURE

The two current model for the conduction in ferromagnets^{25,26} and the corresponding models of the CIP-GMR include three relaxations rates, τ_{\uparrow}^{-1} , τ_{\downarrow}^{-1} , and $\lambda_{\uparrow\downarrow}^{-1}$ [and the three associated characteristic lengths or mean free paths, λ_{\uparrow} , λ_{\downarrow} , and $\lambda_{\uparrow\downarrow}$ (Ref. 27)]. The rates τ_{\uparrow}^{-1} and τ_{\downarrow}^{-1} characterize the relaxation of the momentum to the lattice within each channel, while $\tau_{\uparrow\downarrow}^{-1}$ characterizes the momentum transfer between the two channels (the so-called spin mixing effect). However, for the low temperature limit of the two current model, the usual assumption is $\tau_{\uparrow\downarrow}^{-1}=0$ (no spin mixing). Consequently, there are three characteristic lengths, λ_{\uparrow} , λ_{\downarrow} , and $\lambda_{\uparrow\downarrow}$ at finite temperatures and only two, λ_{\uparrow} and λ_{\downarrow} , in the low temperature limit. In the

models of the CIP-GMR, the assumption $\tau_{\uparrow\downarrow}^{-1}=0$ has been generally assumed valid at any temperature and only a few models introduce a nonzero $\tau_{\uparrow\downarrow}^{-1}$ at finite temperature to describe the temperature dependence of the CIP-GMR.²⁸

For the CPP-GMR the VF model¹³ has been worked out for the low temperature limit and therefore assumes $\tau_{\uparrow\downarrow}^{-1}=0$. In addition, to describe the relaxation of the spin accumulations, it introduces another relaxation rate, the spin relaxation rate τ_{sf}^{-1} . The only scaling length appearing in the final expressions of the CPP-GMR is the spin diffusion length l_{sf} , which is a function of the characteristic lengths λ_{\uparrow} , λ_{\downarrow} , and $\lambda_{\text{sf}}=v_F\tau_{\text{sf}}$. At finite temperatures, it is necessary to introduce the spin mixing effect (momentum transfer) into the VF model and, as described below, $\lambda_{\uparrow\downarrow}$ will also come into play with λ_{\uparrow} , λ_{\downarrow} , and λ_{sf} .

Because the relaxation times $\tau_{\uparrow\downarrow}$ and τ_{sf} are both related to spin flip scattering, there is some confusion between them, so that we begin by explaining in what they differ and why they depend differently on temperature, that is why $\tau_{\uparrow\downarrow}^{-1}(T=0)\approx 0$ and $\tau_{\text{sf}}^{-1}(T=0)\neq 0$.

The relaxation rate $\tau_{\uparrow\downarrow}^{-1}$ characterizes the momentum transfer between the two channels by spin flip scattering, or in other words the relaxation of the magnetization current. *Only the scattering processes which conserve the momentum*, at least partly, contribute to $\tau_{\uparrow\downarrow}^{-1}$; this appears clearly in the usual expressions of $\tau_{\uparrow\downarrow}^{-1}$ or $\rho_{\uparrow\downarrow}$, for example, in Eq. (17) of Ref. 25. Consequently, $\tau_{\uparrow\downarrow}^{-1}$ is zero if, for a given incident wave vector \mathbf{k} , the mean value of the scattered wave vector \mathbf{k}' is zero. At low temperature, for spin-flip scattering by the spin orbit part of impurity or defect potentials (or by the exchange interaction with paramagnetic impurities doping nonmagnetic layers⁶), this condition is approximately obeyed. With also the weakness of the spin-orbit potentials, this explains why $\tau_{\uparrow\downarrow}^{-1}(T=0)$ is assumed to be zero (in fact, in the two current models, the condition $\tau_{\uparrow\downarrow}^{-1}\ll\tau_{\uparrow}^{-1},\tau_{\downarrow}^{-1}$ is sufficient to neglect $\tau_{\uparrow\downarrow}^{-1}$). As T increases, mainly *spin-flip scattering by magnons* comes into play to give $\tau_{\uparrow\downarrow}^{-1}$ a nonzero value, since the electron momentum is partly conserved in electron-magnon collisions: $\mathbf{k}'=\mathbf{k}+\mathbf{q}$, where \mathbf{q} is the magnon wave vector (at relatively low temperatures, q is much smaller than k_F , so that the momentum of the scattered electrons is almost completely transferred to the other channel).

On the other hand, τ_{sf}^{-1} characterizes the relaxation of the out of equilibrium magnetization (or spin accumulation) and *all the spin-flip scattering processes*, with and without momentum conservation, may contribute to τ_{sf}^{-1} providing that the corresponding scattering Hamiltonian does not commute with the total spin of the conduction electron system. At low temperatures, τ_{sf}^{-1} includes contributions from *spin-orbit scattering* by impurities or defects (see Sec. III) and, for nonmagnetic layers doped with paramagnetic impurities,⁶ contributions from *exchange scattering* (see Sec. IV). As T increases, τ_{sf}^{-1} could receive additional contribution from *electron-magnon scattering* in magnetically ordered layers.

The above discussion allows us to classify the several

effects that must be taken into account to describe the temperature dependence of the CPP-GMR.

(a) At finite temperatures, the intrachannel relaxation rates τ_{\uparrow}^{-1} and τ_{\downarrow}^{-1} receive an additional contribution from thermally excited scatterings (phonons, magnons). This can be described in terms of an additional contribution to the resistivity of each channel, that is

$$\rho_{\sigma}(T)=\rho_{\sigma}(T=0)+\delta\rho_{\sigma}(T) \text{ with } \sigma=\uparrow \text{ to } \downarrow \quad (30)$$

in the notation of Ref. 28. In our notation this leads to temperature dependent values of ρ_F^* and β ,

$$\rho_F^*(T)=\frac{\rho_{\uparrow}(T)+\rho_{\downarrow}(T)}{4}, \quad (31)$$

$$\beta(T)=\frac{\rho_{\uparrow}(T)-\rho_{\downarrow}(T)}{\rho_{\uparrow}(T)+\rho_{\downarrow}(T)}. \quad (32)$$

Experimental values of $\delta\rho_{\uparrow}(T)$ and $\delta\rho_{\downarrow}(T)$ for bulk Ni, Fe, and Co can be found in the literature.^{26,29} For the nonmagnetic layer also, $2\rho_N^*(T)=\rho_{\sigma}(T)=\rho_{\sigma}(T=0)+\delta\rho_{\sigma}(T)$, where $\delta\rho_{\sigma}(T)$ is independent of σ and is twice the phonon resistivity of the bulk metal $\delta\rho_N(T)$.

In principle, the spin dependent interface resistances r_{\uparrow} and r_{\downarrow} involved in the VF model should also receive some temperature dependent contributions due to interface phonons and magnons. For simplicity we neglect this temperature dependent of r_{\uparrow} and r_{\downarrow} but it could be included straightforwardly in the calculation.

(b) Electron-magnon scattering not only contributes to $\delta\rho_{\uparrow}(T)$ and $\delta\rho_{\downarrow}(T)$ but also to the spin mixing rate $\tau_{\uparrow\downarrow}^{-1}$ or, in terms of resistivity, to the spin mixing resistivity $\rho_{\uparrow\downarrow}(T)$.^{25,26} The spin mixing tends to equalize the two currents and lowers the GMR. Experimental data on $\rho_{\uparrow\downarrow}(T)$ for Ni, Fe, and Co can be found in the literature.^{25,26,29}

(c) Spin slip electron-magnon scattering could also contribute to the spin relaxation rate τ_{sf}^{-1} and therefore to shorten the spin-diffusion length in the magnetic layers.

A. Temperature dependence due to spin mixing and temperature dependent spin resistivities

In most experimental systems,⁴⁻⁶ l_{sf} exceeds 10^3 Å and is much larger than the layer thicknesses. The spin-diffusion length in the ferromagnetic layers, $l_{\text{sf}}^{(F)}$, will be shortened by electron-magnon scattering but, from the conclusions of Sec. II, the CPP-GMR is reduced only when the spin diffusion length is shortened to the order of magnitude of the layer thickness (and, moreover, the effect is less severe when the reduction is for $l_{\text{sf}}^{(F)}$). Thus we postpone the discussion of the effects due to the shortening of $l_{\text{sf}}^{(F)}$ to Sec. V B. In this section, we consider the case where the shortening is not sufficient to go outside the long spin-diffusion-length limit and we discuss the temperature dependence due to $\delta\rho_{\sigma}(T)$ and $\rho_{\uparrow\downarrow}(T)$.³¹

In the long spin-diffusion-length limit of the VF model, the current densities J_+ and J_- for the two absolute spin directions are constant throughout the multilayer and can be determined by averaging all the scattering probabilities in each channel. The voltage drop V across the

multilayer is thus related to J_+ and J_- by the usual coupled equations of the two current model,^{25,26}

$$\begin{aligned} V &= R_+ J_+ + R_{(+,-)}(J_+ - J_-), \\ V &= R_- J_- + R_{(+,-)}(J_- - J_+), \end{aligned} \quad (33)$$

with, in the notation of Sec. II,

$$R_{(+,-)} = M t_F \rho_{\uparrow\downarrow}(T) \quad (34)$$

and, in the case of antiparallel (or random) arrangement of the layer moments,

$$R_{\pm}^{(\text{AP})} = R_{\pm}^{(\text{AP})} = M [2t_F \rho_F^*(T) + 2t_N \rho_N^*(T) + 4r_b^*], \quad (35)$$

while, in the case of parallel arrangement,

$$\begin{aligned} R_{\pm}^{(\text{P})} &= M [2t_F \rho_F^*(T)(1 \mp \beta(T)) \\ &\quad + 2t_N \rho_N^*(T) + 4r_b^*(1 \mp \gamma)]. \end{aligned} \quad (36)$$

The two terms in the right side of Eq. (33) express the intrachannel relaxation of the momentum and the interchannel momentum transfer, respectively. Equations (34)–(36) simply mean that the relaxation and transfer rates are averaged in each channel. The resistance of a unit surface of the multilayer, that is $R = V/(J_+ + J_-)$, is obtained by solving Eqs. (33) and this leads to the familiar expression^{25,26} of the two current model,

$$R = \frac{R_+ R_- + R_{(+,-)}(R_+ + R_-)}{R_+ + R_- + 4R_{(+,-)}}. \quad (37)$$

The resistance $R^{(\text{AP})}$ and $R^{(\text{P})}$ for the antiparallel and parallel arrangements are then derived from Eqs. (34)–(36) and we obtain

$$\begin{aligned} \sqrt{[R^{(\text{AP})} - R^{(\text{P})}]R^{(\text{AP})}} \\ = \frac{M[\beta(T)t_F \rho_F^*(T) + 2\gamma r_b^*]}{1 + M \frac{t_F \rho_{\uparrow\downarrow}(T)}{R^{(\text{AP})}}}. \end{aligned} \quad (38)$$

Compared to the similar expressions for the low temperature limit, Eq. (3), the only differences are ρ_F^* and ρ_N^* are replaced by $\rho_F^*(T) = \rho_F^* + [\delta\rho_{\uparrow}(T) + \delta\rho_{\downarrow}(T)]/4$ [see Eq. (31)] and $\rho_N^*(T) = \rho_N^* + \delta\rho_{\sigma}(T)/2 = \rho_N^* + \delta\rho_N(T)$; β is replaced by $\beta(T)$ [Eq. (32)]; and a reduction factor $1/[1 + M t_F \rho_{\uparrow\downarrow}(T)/R^{(\text{AP})}]$ expresses the spin mixing effects.

The variation of $\sqrt{[R^{(\text{AP})} - R^{(\text{P})}]R^{(\text{AP})}}$ with T results from several competing effects. The increase of $\rho_F^*(T)$ with T tends to increase it but, if the spin asymmetry between $\delta\rho_{\uparrow}(T)$ and $\delta\rho_{\downarrow}(T)$ is less pronounced than that between the low temperature resistivities ρ_{\uparrow} and ρ_{\downarrow} , the resulting decrease of $\beta(T)$ goes in the opposite direction. Also the increase of $\rho_{\uparrow\downarrow}(T)$ with T in the denominator tends to decrease the square root. In addition, the variation is no longer linear in M since M is also involved in the denominator.

Starting from the low temperature values of ρ_F^* , β , ρ_N^* , r_b , and γ derived by Pratt *et al.*⁶ for Co/Cu and introducing values of $\delta\rho_{\uparrow}(T)$, $\delta\rho_{\downarrow}(T)$, and $\rho_{\uparrow\downarrow}(T)$ derived for

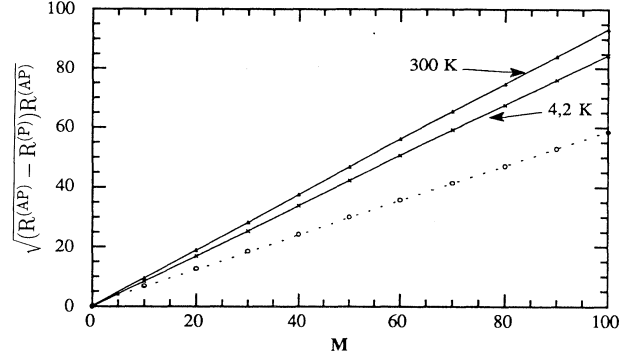


FIG. 3. $\sqrt{[R^{(\text{AP})} - R^{(\text{P})}]R^{(\text{AP})}}$ versus the number of bilayers M calculated for Co/Cu multilayers at 4.2 and 300 K. The calculation is performed in the long spin-diffusion-length limit by using Eq. (38) which takes into account phonon and magnon intrachannel resistivities, and also the interchannel spin mixing term. The curve for 4.2 K is calculated for $\delta\rho_N^*(4.2) = \delta\rho_F^*(4.2) = \rho_{\uparrow\downarrow}(4.2)$; the curve for 300 K is calculated by using values of $\delta\rho_N^*(300)$, $\delta\rho_F^*(300)$, $\beta(300)$, and $\rho_{\uparrow\downarrow}(300)$ derived from data on bulk metals or alloys (Refs. 28 and 29). The dashed line is calculated for an arbitrarily large value of $\rho_{\uparrow\downarrow}$ [ten times $\rho_{\uparrow\downarrow}(300)$] but, even with such a large value of $\rho_{\uparrow\downarrow}$, the deviation from linearity is still negligible.

bulk Co (Ref. 29) and the phonon resistivity $\delta\rho_N(T)$ for bulk Cu,^{29,30} we have calculated $\sqrt{[R^{(\text{AP})} - R^{(\text{P})}]R^{(\text{AP})}}$ at 300 K as a function of the numbers of bilayers M for Co/Cu multilayers with a total thickness $L = 7200 \text{ \AA}$, $t_{\text{Co}} = 15 \text{ \AA}$, and $t_{\text{Cu}} = L/M - t_{\text{Co}}$.³¹ As shown in Fig. 3 the values of $\sqrt{[R^{(\text{AP})} - R^{(\text{P})}]R^{(\text{AP})}}$ at 300 K are slightly above those at $T = 0$. The deviation from a linear variation is small and almost negligible. A similar enhancement of the slope of the square root plot has been observed in measurements on Co/Cu by Gijs.³² A more pronounced deviation from linearity can be obtained only with much higher values of $\rho_{\uparrow\downarrow}$ (300 K). The dashed curve has been obtained by introducing arbitrarily a value of $\rho_{\uparrow\downarrow}(300 \text{ K})$ ten times larger than the bulk one. Even with this large value of $\rho_{\uparrow\downarrow}$, the deviation from linearity is still extremely small.

From the above equations, we have also calculated the temperature dependence of $[R^{(\text{AP})} - R^{(\text{P})}]/R^{(\text{P})}$ for Co 15 \AA /Cu 20 \AA using the same low temperature parameters of Pratt *et al.*⁵ and the same experimental data as above for $\delta\rho_{\uparrow}(T)$, $\delta\rho_{\downarrow}(T)$, and $\rho_{\uparrow\downarrow}(T)$ in Co and for the phonon resistivity in Cu. In Fig. 4 we show the corresponding variation of the CPP-GMR ratio with T . This variation can be compared with the variation of CIP-GMR ratio calculated in a semiclassical model for the same structure.^{28,33} The temperature variation of the MR is relatively weak in both geometries, in agreement with the experimental data.^{28,32} More precisely, the experimental temperature dependences are slightly more pronounced than the calculated ones, which could be due to enhanced spin fluctuations at the interfaces. This could be taken

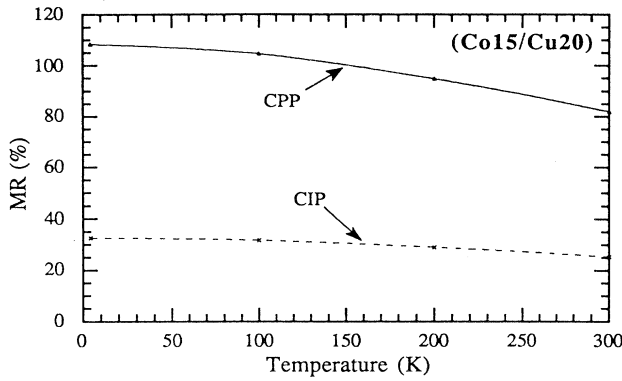


FIG. 4. Variation with temperature of the CPP- and CIP-MR for a Co 15 Å/Cu 20 Å multilayer calculated (as described in the text) from values of $\delta\rho_N^*(T)$, $\delta\rho_F^*(T)$, $\beta(T)$, and $\rho_{\uparrow\downarrow}(T)$ derived from data on bulk metals and alloys (Refs. 29 and 30). The variation is somewhat smaller than the experimental one (Refs. 28 and 32), which suggest an additional contribution to $\delta\rho^*(T)$ and $\rho_{\uparrow\downarrow}(T)$ from the interfaces.

into account by introducing temperature-dependent interface resistance $\delta r_{\uparrow}(T)$, $\delta r_{\downarrow}(T)$, and $\delta r_{\uparrow,\downarrow}(T)$.

B. Temperature dependence of the spin-diffusion length in the ferromagnetic layers

In order to consider the influence of the spin fluctuations on the conduction electron spin-diffusion length in the ferromagnetic layers, we will adopt the physical picture of slightly polarized, small effective mass “*s*” electrons (mainly responsible for the current conduction) and heavily polarized, large effective mass “*d*” electrons (mainly responsible for the spontaneous magnetization) coexisting at the Fermi level. We will also assume an *s-d* exchange interaction of the kind in Eq. (15).

Within this model, at nonzero temperature the thermally excited magnons in the *d* subsystem will scatter the conduction electrons. But, because the *s-d* Hamiltonian (15) conserve the total spin of the system *s* + *d* electrons, it is clear that the spin-flip part of these scatterings (due to the $s_-S_+ + s_+S_-$ terms of the Hamiltonian) will not relax the *s* electron spin accumulation directly to the lattice, but will rather allow exchange of spin accumulation between the *s* and *d* subsystems. Anyhow, this is only an additional mechanism of equalization of the chemical potential shifts between the *s* and *d* bands, since *s-d* elastic scatterings on impurities and defects is an even more efficient mechanism already present at low temperature. With, at any temperature, the spin accumulation spread in both bands, its relaxation to the lattice is always controlled by the almost temperature independent spin-orbit scattering (in both bands, by impurity, defects, phonons etc.).

In conclusion, we guess that electron-magnon scatterings do not provide an additional efficient mechanism of relaxation of spin accumulation to the lattice, and should not affect significantly the spin-diffusion length. The temperature dependence of the CPP-MR should be predom-

inantly due to the spin-mixing effect described in Sec. V A.

VI. SUMMARY AND CONCLUSIONS

The spin-diffusion lengths $l_{sf}^{(N)}$ and $l_{sf}^{(F)}$ are the scaling lengths of the perpendicular transport in magnetic multilayers and this leads to very simple linear variations, Eq. (3) or Eqs. (4) and (5), when the thicknesses (t_F, t_N) are much smaller than the spin-diffusion lengths (SDL). Such linear variations have been observed in extensive measurements at Michigan State University and are useful to separate simply the bulk and interface contributions.^{4–6} Out of the long spin-diffusion-length limit, the CPP-MR is given by Eqs. (6)–(8). In Sec. II we have described the corresponding behavior, and in Figs. 1 and 2 we have illustrated how the CPP-MR is reduced and departs from linear variations when one goes away from the long spin-diffusion-length limit.

Bass *et al.*⁶ have confirmed this behavior at finite SDL by adding Pt or Mn impurities in Co/Ag or Co/Cu multilayers to shorten the spin-diffusion length, $l_{sf}^{(N)}$, in the nonmagnetic layers. In Sec. III we have calculated the shortening of $l_{sf}^{(N)}$ by impurities with large spin-orbit interactions, and shown that the values of $l_{sf}^{(N)}$ predicted for Pt impurities are in good agreement with those derived by Bass *et al.*⁶ In Sec. IV we have calculated the shortening of $l_{sf}^{(N)}$ by paramagnetic impurities in Cu and accounted for experimental results of Bass *et al.*⁶ on Co/CuMn multilayers at 4.2 K. In addition we predict how the effect of Mn impurities should be reduced by an increase of temperature. Section V is devoted to the temperature dependence of the CPP-MR. In Sec. V A we suppose that the spin-diffusion lengths remain much longer than the thicknesses at any temperature, and we calculate the variation with temperature due to spin mixing of the spin \uparrow and spin \downarrow currents. We apply our results to the case of Co/Cu multilayers and we find a relatively weak temperature dependence for both the CPP and CIP-MR, in agreement with recent experimental results.⁷ In Sec. V B, it is furthermore shown that the electron-magnon scattering can hardly be considered to affect significantly this weak temperature dependence through spin diffusion length $l_{sf}^{(F)}$ shortening.

Our calculations have been applied mainly to Co/Cu or Co/Ag multilayers doped with Pt or Mn impurities. Similar analyses should be of interest in multilayers doped with other types of impurities for extensive determination of spin-flip cross section.

ACKNOWLEDGMENTS

We acknowledge fruitful discussions with J. Bass, W. P. Pratt, P. A. Schroeder, M. Gijs, P. Monod, and H. Hurdequint. We also thank the Michigan State University group for communicating unpublished data. Our collaboration was supported by Grant No. A1 0693 from the CNRS and by companion Grant No. INT-92-16909 of the U.S.-NSF. We also acknowledge support from the European Union through the Esprit project No. BRA 6146 and Brite Euram project No. BRE2-0546.

- ¹M. N. Baibich, J. M. Broto, A. Fert, F. Nguyen Van Dau, F. Petroff, P. Etienne, G. Creuzet, A. Friederich, and J. Chazelas, *Phys. Rev. Lett.* **61**, 2472 (1988).
- ²G. Binash, P. Grunberg, F. Saurenbach, and W. Zinn, *Phys. Rev. B* **39**, 4828 (1989).
- ³W. P. Pratt, Jr., S. F. Lee, J. M. Slaughter, R. Loloee, P. A. Schroeder, and J. Bass, *Phys. Rev. Lett.* **66**, 3060 (1991).
- ⁴S. F. Lee, W. P. Pratt, Q. Yang, P. Holody, R. Loloee, P. A. Schroeder, and J. Bass, *J. Magn. Magn. Mater.* **118**, 1 (1993).
- ⁵W. P. Pratt, Jr., S. F. Lee, P. Holody, Q. Yang, R. Loloee, J. Bass, and P. A. Schroeder, *J. Magn. Magn. Mater.* **126**, 406 (1993); P. A. Schroeder, J. Bass, P. Holody, S. F. Lee, R. Loloee, W. P. Pratt, and Q. Yang, in *Magnetism and Structure in Systems of Reduced Dimension*, Vol. 309 of *NATO Advanced Study Institute, Series B: Physics*, edited by R. F. Farrow *et al.* (Plenum, New York, 1993), p. 129.
- ⁶Q. Yang, P. Holody, S. F. Lee, L. L. Henry, R. Loloee, P. A. Schroeder, W. P. Pratt, and J. Bass, *Phys. Rev. Lett.* **72**, 3274 (1994); J. Bass, Q. Yang, S. F. Lee, P. Holody, R. Loloee, P. A. Schroeder, and W. P. Pratt, *J. Appl. Phys.* **75**, 6699 (1994).
- ⁷M. A. M. Gijs, S. K. Lenczowski, and J. B. Giesbers, *Phys. Rev. Lett.* **70**, 3373 (1993).
- ⁸M. Johnson, *Phys. Rev. Lett.* **67**, 3594 (1991).
- ⁹S. Zhang and P. M. Levy, *J. Appl. Phys.* **69**, 4786 (1991); H. E. Camblong, S. Zhang, and P. M. Levy, *Phys. Rev. B* **47**, 4735 (1993).
- ¹⁰G. E. W. Bauer, *Phys. Rev. Lett.* **69**, 1676 (1992).
- ¹¹J. Inoue, H. Itoh, S. Maekawa, *J. Magn. Magn. Mater.* **126**, 413 (1993); Y. Asano, A. Oguri, and S. Maekawa, *Phys. Rev. B* **48**, 6192 (1993).
- ¹²A. Fert, T. Valet, and J. Barnas, *J. Appl. Phys.* **75**, 6693 (1994); A. Fert, A. Barthe'lemy, P. Galtier, P. Holody, R. Loloee, R. Morel, F. Pétroff, P. Schroeder, L. B. Steren, T. Valet, *Mat. Sci. Eng. B* **34**, 1 (1995).
- ¹³T. Valet and A. Fert, *Phys. Rev. B* **48**, 7099 (1993).
- ¹⁴P. Monod and S. Schultz, *J. Phys. (Paris)* **43**, 393 (1992).
- ¹⁵Y. Yafet, *J. Appl. Phys.* **39**, 853 (1968); **42**, 1564 (1971).
- ¹⁶J. S. Griffith, *The Theory of Transition Metal Ions* (Cambridge University Press, Cambridge, England, 1961), p. 113.
- ¹⁷J. Cottet, Ph.D. thesis, Université de Genève, 1970.
- ¹⁸J. Bass, in *Metals: Electronic Transport Phenomena*, edited by K. H. Hellwege and J. L. Olsen, Landolt-Börnstein, New Series, Group 3, Vol. 15, Pt.a (Springer-Verlag, Berlin, 1982).
- ¹⁹A. C. Gossard, T. Kometai, and J. H. Wernick, *J. Appl. Phys.* **39**, 849 (1968).
- ²⁰There is a factor of 2 between the VF notation in Refs. 12 and 13 and the usual notation for the ESR problem: if τ_{sf}^{-1} is the spin-flip rate (notation of Valet and Fert for the spin-flip processes due to spin-orbit interaction), the relaxation of the out of equilibrium magnetization is written as $d(\Delta M_s)/dt = -2\mu_B(n_+ - n_-)/\tau_{sf} = -2\Delta M_s/\tau_{sf}$ while in the usual notation of ESR one writes $d(\Delta M_s)/dt = -\Delta M_s/\tau_{sf}$. Consequently τ_{sf}^{-1} equals $2\tau_{sl}^{-1}$. This accounts for the factor 4π turning out in Eq. (21) or (22) for τ_{sf}^{-1} instead of the factor 8π in the corresponding expression of τ_{sd}^{-1} , Eq. (16).
- ²¹A. Overhauser, *Phys. Rev.* **89**, 689 (1953).
- ²²J. Korringa, *Physica* **16**, 601 (1950).
- ²³A. Fert, A. Friederich, and A. Hamzic, *J. Magn. Magn. Mater.* **24**, 231 (1981).
- ²⁴H. Hurdequint, Ph.D. thesis, Orsay, 1981, p. V23 unpublished; D. Davidov, C. Rettori, R. Orbach, A. Dixon, and E. P. Chock, *Phys. Rev. B* **11**, 3546 (1975).
- ²⁵A. Fert and I. A. Campbell, *J. Phys. F* **6**, 849 (1976).
- ²⁶I. A. Campbell and A. Fert, in *Ferromagnetic Materials*, edited by E. P. Wohlfarth (North-Holland, Amsterdam, 1982), Vol. 3, p. 747.
- ²⁷The mean free path and the resistivity are related to the relaxation times by $\lambda = v_F \tau$ and $\rho = m / (ne^2 \tau)$, where n is the number of electrons per unit volume in the corresponding channel.
- ²⁸J. L. Duvail, A. Fert, L. G. Pereira, and D. K. Lottis, *J. Appl. Phys.* **75**, 7070 (1994).
- ²⁹B. Loegel and F. Gautier, *J. Phys. Chem. Solids* **32**, 2732 (1971).
- ³⁰G. K. White and S. B. Woods, *Philos. Trans. R. Soc. London Ser. A* **251**, 273 (1959).
- ³¹For a similar calculation introducing experimental data on $\delta\rho_{\uparrow}(T)$, $\delta\rho_{\downarrow}(T)$, and $\rho_{\uparrow\downarrow}(T)$ in a calculation of CIP-GMR, see Ref. 28.
- ³²M. Gijs, *Mat. Sci. Eng. B* **31**, 85 (1995).
- ³³In the semiclassical model used for the calculation of the CIP-MR, the interface scattering is treated by introducing a 2 Å thick interface layer with a resistivity excess chosen to give back the interface resistances r_{\uparrow} and r_{\downarrow} of Pratt *et al.*⁵ in perpendicular transport. The semiclassical calculation is described in Ref. 28.